

See discussions, stats, and author profiles for this publication at: <https://www.researchgate.net/publication/236095627>

Kinetic, Electrochemical, and Microscopic Characterization of the Thermophilic, Anode-Respiring Bacterium *Thermincola ferriacetica*

ARTICLE in ENVIRONMENTAL SCIENCE & TECHNOLOGY · APRIL 2013

Impact Factor: 5.33 · DOI: 10.1021/es400321c · Source: PubMed

CITATIONS

20

READS

76

6 AUTHORS, INCLUDING:



[Prathap Parameswaran](#)

Kansas State University

46 PUBLICATIONS 1,745 CITATIONS

[SEE PROFILE](#)



[Sudeep C Popat](#)

Arizona State University

21 PUBLICATIONS 212 CITATIONS

[SEE PROFILE](#)



[Bradley Lusk](#)

Arizona State University

5 PUBLICATIONS 20 CITATIONS

[SEE PROFILE](#)



[Bruce Rittmann](#)

Arizona State University

518 PUBLICATIONS 17,210 CITATIONS

[SEE PROFILE](#)

Kinetic, Electrochemical, and Microscopic Characterization of the Thermophilic, Anode-Respiring Bacterium *Thermincola ferriacetica*

Prathap Parameswaran,^{*,†} Tyson Bry,^{†,§} Sudeep C. Popat,[†] Bradley G. Lusk,[†] Bruce E. Rittmann,^{†,§} and César I. Torres^{†,‡}

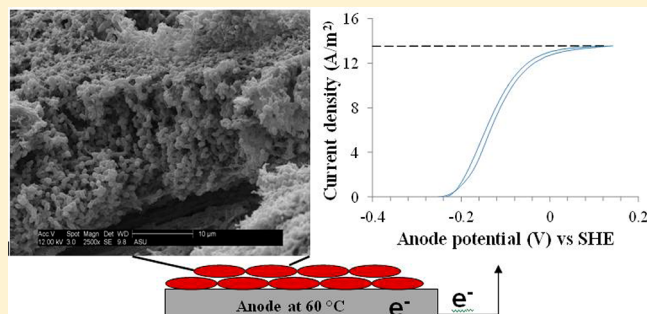
[†]Swette Center for Environmental Biotechnology, The Biodesign Institute at Arizona State University, P.O. Box 875701, Tempe, Arizona 85287, United States

[‡]School for Engineering of Matter, Transport and Energy, Arizona State University, Tempe, Arizona, United States

[§]School of Sustainable Engineering and the Built Environment, Arizona State University, Tempe, Arizona, United States

Supporting Information

ABSTRACT: *Thermincola ferriacetica* is a recently isolated thermophilic, dissimilatory Fe(III)-reducing, Gram-positive bacterium with capability to generate electrical current via anode respiration. Our goals were to determine the maximum rates of anode respiration by *T. ferriacetica* and to perform a detailed microscopic and electrochemical characterization of the biofilm anode. *T. ferriacetica* DSM 14005 was grown at 60 °C on graphite-rod anodes poised at -0.06 V (vs) SHE in duplicate microbial electrolysis cells (MECs). The cultures grew rapidly until they achieved a sustained current density of 7–8 A m⁻² with only 10 mM bicarbonate buffer and an average Coulombic Efficiency (CE) of 93%. Cyclic voltammetry performed at maximum current density revealed a Nernst–Monod response with a half saturation potential (E_{KA}) of -0.127 V (vs) SHE. Confocal microscopy images revealed a thick layer of actively respiring cells of *T. ferriacetica* (~38 μm), which is the first documentation for a gram positive anode respiring bacterium (ARB). Scanning electron microscopy showed a well-developed biofilm with a very dense network of extracellular appendages similar to *Geobacter* biofilms. The high current densities, a thick biofilm (~38 μm) with multiple layers of active cells, and Nernst–Monod behavior support extracellular electron transfer (EET) through a solid conductive matrix – the first such observation for Gram-positive bacteria. Operating with a controlled anode potential enabled us to grow *T. ferriacetica* that can use a solid conductive matrix resulting in high current densities that are promising for MXC applications.



INTRODUCTION

Microbial electrochemical cells (MXCs) have emerged as an option for sustainable production of renewable electric power, hydrogen gas, hydrogen peroxide, caustic soda, and other products from organic waste streams.^{1–4} Anode-respiring bacteria (ARB) represent a unique group of anaerobic microorganisms that perform extracellular electron transfer (EET) to a solid electrode in MXCs, thus producing electrical current.⁵ Although several ARB have been found in globally diverse environmental matrices,^{6–9} only a few strains from *Geobacter* and *Shewanella* genera are well-studied ARB on MXC anodes.^{10,11} *Geobacter* spp. produces 6–10 A m⁻² on flat planar anode surfaces^{12,14} and up to 66 A m⁻² on non-3D microelectrodes,¹⁵ whereas *Shewanella* spp. produces 0.008–0.97 A m⁻² on planar and microporous surfaces.^{16,17}

Three general mechanisms can be utilized by ARB for EET to an anode: (1) direct contact through outer membrane proteins from a monolayer of cells on the anode, (2) diffusion of soluble electron shuttles between the cells and the anode, and (3) electron transport through solid components of an

extracellular biofilm matrix involving multiple layers of actively respiring cells.⁵ Direct contact alone cannot support the high current densities observed in *Geobacter* spp. due to a limited number of cells that can form a monolayer, whereas electron transfer through soluble electron shuttles is impeded by their slow diffusion at commonly observed concentrations.^{10,18} Thus, a solid conductive matrix is the only means for an ARB to achieve high current densities (>0.3 A m⁻²). Two theories are proposed to explain EET via a solid conductive matrix in *Geobacter sulfurreducens*: electron hopping through redox proteins, or electron superexchange,¹⁰ and electron transfer through conductive pili that possess tunable metallic-like conductivity.¹⁹ Given our limited knowledge about EET in thermophilic ARB, we use the more general term of a solid conductive matrix.

Received: January 21, 2013

Revised: March 30, 2013

Accepted: April 1, 2013

Published: April 1, 2013



Thermophilic ARB have only recently become an active area of research. *Thermincola ferriacetica*^{20,21} and *Thermincola potens*^{22,23} are two thermophilic, Gram-positive, metal-reducing bacteria able to generate current from acetate on anodes of microbial fuel cells (MFCs). Current densities generated by these strains were reported to be up to 1 A m⁻². Thermophilic mixed cultures dominated by the *Bacteroidetes* genus also produced current densities of around 2 A m⁻² in MFCs fed with alcohol distillery wastewater.²⁴ Recent research has shed light on EET mechanisms used by the Gram-positive thermophilic bacterium *T. potens*. It suggests a direct-contact mechanism for Fe(III) reduction and anode respiration with no definitive evidence for long-range electron transport.^{23,25} Initial investigations on *T. ferriacetica* biofilms produced low current densities of 0.5 A m⁻²²¹ in MFC operation, which is low enough to be produced by a monolayer of cells requiring direct contact with the anode.⁵

The discovery of thermophilic ARB, specifically from the *Thermincola* genus, has important scientific and technological relevance. First, *Thermincola* sp. are Gram-positive bacteria and should significantly differ in their extracellular and membrane-bound proteins compared to well-known Gram-negative ARB (e.g., *G. sulfurreducens*, *S. oneidensis*). Whereas so far only direct contact by a monolayer of cells has been suggested as the mechanism for anode respiration in Gram-positive thermophilic ARB, it remains to be seen if they can also form thick, high current density producing biofilms like some Gram-negative bacteria. Second, thermophilic temperatures provide faster kinetics through reduction of the exponential of activation energy term, exp (-E_a/T), as described by the Arrhenius equation, within the temperature range in which the enzymes are stable; especially of value is the enhanced rate of hydrolysis of complex organic matter that could be achieved at higher temperatures.^{26–28}

Previous studies show that thermophilic ARB cannot produce current densities comparable to those generated by mesophilic counterparts, such as *Geobacter* spp, under the MFC mode of operation. Several factors have hampered the evaluation of the kinetics of thermophilic ARB in previous studies. The first is the lack of a controlled anode potential, an important variable for selecting efficient ARB.^{8,12,29} The second is the presence of oxygen or other terminal electron acceptors at the cathode, which can leak into the anode and inhibit the thermophilic ARB or divert electrons away from anode respiration. Both complications can be avoided when the biofilm anode is operated in a two-chamber microbial electrolysis cell (MEC) for evaluating the maximum abilities of *Thermincola* on the anode. It is equally important to identify what EET mechanism Gram-positive thermophilic ARB use to produce high current densities. We already know that direct contact would not be sufficient if thermophilic ARB were to produce relatively high current densities: greater than the 0.3 A m⁻² cut off value for mesophilic ARB and possibly a slightly higher cutoff due to the faster reaction kinetics at higher temperature.²¹ This means they would have to form a conductive biofilm much thicker than a monolayer to produce higher current densities. Hence, electrochemical and microscopic characterizations are essential to define the EET mechanisms for Gram-positive bacteria and to compare them with *Geobacter* spp.

The goals of our study are 2-fold. The first is to evaluate the maximum current-production capability of *T. ferriacetica* at the biofilm anode during MEC mode of operation. The second

goal is to combine electrochemical, kinetic, and microscopic characterization of *T. ferriacetica* to determine key kinetic parameters and identify their EET mechanism.

MATERIALS AND METHODS

Growth of *Thermincola ferriacetica* DSMZ 14005 with Fe(III) Oxide and AQDS. We obtained a pure culture of *T. ferriacetica* strain 14005 from DSMZ, Braunschweig, Germany, and cultivated the strain in serum bottles using the medium conditions prescribed by DSMZ. The medium consisted of the following in 1 L of deionized water: 0.33 g each of NH₄Cl, KH₂PO₄, MgCl₂·6H₂O, CaCl₂·2H₂O, and KCl; 0.05 g yeast extract; 1 mL selenite-tungstate stock solution (prepared by dissolving 3 mg Na₂SeO₃·5H₂O, 4 mg Na₂WO₄·2H₂O, and 0.5 g NaOH in 1 L distilled water); 0.7 g NaHCO₃; 2.72 g NaAc·3H₂O; 10 mL ATCC vitamin solution; and 10 mL trace elements solution. The trace elements solution consisted of the following ingredients in 1 L deionized water: 1.5 g nitrilotriacetic acid, 3 g MgSO₄·7H₂O, 0.5 g MnSO₄·H₂O, 1 g NaCl, 0.1 g FeSO₄·7, 0.18 g COSO₄·7H₂O, 0.1 g CaCl₂. Two H₂O, 0.18 g ZnSO₄·7H₂O, 0.01 g CuSO₄·5H₂O, 0.02 g KAl(SO₄)₂·12H₂O, 0.01 g H₃BO₃, 0.01 g Na₂MoO₄·2H₂O, 0.03 g NiCl₂·6H₂O, and 0.3 mg Na₂SeO₃·5 H₂O. We grew the pure cultures in this medium using either 10 mM Fe(OH)₃ or 25 mM AQDS as the electron acceptor in batch serum bottles maintained at 60 °C. We monitored cell growth by tracking acetate depletion and reduction of the electron acceptor. We serially transferred the cultures to serum bottles to develop a stock culture to use as inoculum for the MEC experiments.

MEC Construction and Operation. We performed duplicate batch experiments at two different times, both with a duration of about one month, using dual-chamber MECs constructed as described earlier.³⁰ The anode electrode was comprised of two graphite rods with a total surface area of 7.6 cm² (each 4 cm long and 0.3 cm in diameter). We poised the anode at -0.06 V (vs) Standard Hydrogen Electrode (SHE) using a potentiostat (VMP3, BioLogic, USA), based on the temperature corrected environmental midpoint potential for solid ferrihydrites (Fe^{III}) reduction to Fe^{II}³¹ prior cyclic voltammetry (CV) performed on *T. ferriacetica* in our lab (data not shown), and from a practical perspective to obtain maximum current density at as low of an anode potential possible. We report all values for the anode potential normalized to the standard hydrogen electrode (SHE). We used Ag/AgCl reference electrodes which are -0.242 V versus SHE at 60 °C in our media composition. We determined the conversion by measuring the difference in potential between an Ag/AgCl reference electrode placed in a two-chambered cell containing our media in one chamber and 1 M KCl in the other; we added the measured potential to the published value for the potential of Ag/AgCl reference electrode in 1 M KCl at 60 °C.³² We used the DSMZ culture media for the anode compartment but excluded the electron acceptor. We harvested 20 mL of Fe(OH)₃-grown cells from serum bottles at the end of log phase to serve as the inoculum for the anode chamber, and we added 80 mL of the spent medium from the same bottle. NaHCO₃ (10 mM) was the buffer, acetate (35 mM) was the electron donor, and the initial pH was 6.95. The cathode chamber contained 325 mL of 0.1 N NaOH solution at pH 13, and it was separated from the anode chamber using an anion exchange membrane (AMI 7001, Membranes International, Glen Rock, NJ). The MECs were placed in a 60 °C incubator.

Coulombic Efficiency. Coulombic efficiency (CE) was calculated by dividing the measured electrons recovered as current at the anode by the measured electrons removed from the electron donor in the anode chamber between the start and end of each batch experiment. To measure the acetate concentration, we collected 1 mL of anode medium at both time points, filtered them through a 0.2 μm filter, and assayed acetate using an HPLC (Shimadzu, USA) equipped with an Aminex HPX-87H column.³⁰

Growth-Rate Experiments. To determine the growth rate and doubling times of *T. ferriacetica* as a biofilm anode, we performed three separate batch MEC experiments using conditions similar to those described in the previous section. Using one of the MECs described above, we removed all attached cells from the 0.25 cm^2 of biofilm and suspended them in 1 mL of medium. We then used 100 μL of this 1 mL cell suspension as inoculum for the growth rate experiments. This small inoculum size was required for accurately measuring the ARB growth rate on the anode³³ as it eliminated current production solely from initial attachment of a large number of metabolically active cells. We focused on current generation during the first 12 h of exponential growth of the *T. ferriacetica* biofilm anode to estimate the doubling time and the specific growth rate because the current is proportional to the mass of ARB when they are not limited by substrate or electron transfer. We note that this is an indirect method to determine growth rate without actual measurement of cells or protein content.

Cyclic Voltammetry. We performed cyclic voltammetry (CV) scans when the ARB were oxidizing an electron donor (acetate). This is usually referred to as catalytic or turnover CV,³⁴ and the CV response is an aggregate of multiple turnovers of each redox species. We performed triplicate CV scans on *T. ferriacetica* biofilm anodes at maximum current density, which was achieved by supplying excess acetate. We performed the scans at 1 mV s^{-1} in the potential range of -0.45 to +0.25 V (vs) SHE and fit the experimental CV to the Nernst–Monod equation³⁵ with $n = 1$, which represents the electrochemical behavior of *Geobacter* spp.³⁶

In the absence of an exogenous electron donor, properties related to interfacial electron transfer between multiple redox species or redox centers of ARB can be probed without interference from the large flow of electrons from oxidation of the exogenous electron donor. These CVs, often referred to as nonturnover CVs,³⁴ were performed at the end of batch MEC experiments when the current density dropped below 0.1 A m^{-2} . We added acetate-free medium and conducted the CV scans at 1 and 10 mV s^{-1} . We also performed CVs on the bare anode electrodes in the same spent medium to confirm the absence of any background redox response from the electrode or the media.

Estimating Apparent Kinetic Parameters for the *T. ferriacetica* Biofilm Anode. The maximum current density ($j_{\max,\text{app}}$) is related to the amount of biofilm accumulation by the following equation³⁷

$$j_{\max,\text{app}} = 0.14f_e^{\circ} q_{\max,\text{app}} X_f L_f = 0.14\text{CE} q_{\max,\text{app}} X_f L_f \quad (1)$$

where 0.14 is conversion factor for changing g COD $\text{m}^{-2} \text{d}^{-1}$ to A m^{-2} , f_e° is the fraction of electrons utilized from the donor that are resired to the anode which is equal to Coulombic efficiency (CE), $q_{\max,\text{app}}$ is the maximum specific substrate utilization rate (g COD g VS⁻¹ d⁻¹), X_f is the active ARB

concentration (g VS m^{-3}), and L_f is the biofilm thickness (m).³⁷ We measured L_f using a ZEISS confocal laser scanning microscope (CSLM) after applying LIVE/DEAD (BacLight Cell vitality kit, Invitrogen, USA) staining of the biofilm anode at the end of a batch MEC experiment, that is, biofilm samples taken at 27 days in run 2.

We determined the fraction of electron equivalents used for energy generation via anode respiration (f_e°) directly from CE. Because the only sinks for electrons removed from the donor were electric current and biomass synthesis and soluble microbial products (SMP), we calculated f_s° , the fraction of donor electrons used in synthesis, from $f_e^{\circ} + f_s^{\circ} = 1$ or $f_s^{\circ} = 1 - \text{CE}$. Then, the Y value for *T. ferriacetica* is proportional to f_s° :

$$Y = \frac{f_s^{\circ} \left(\frac{1}{20} \right) (113 \text{ g cells/mol cells})}{\left(\frac{1}{8} \right) (61 \text{ g mole}^{-1})} = 0.74 f_s^{\circ} \quad (2)$$

where 113 (g cells/mol cells) is the molecular weight for bacteria biomass according to the formula C₅H₇O₂N (55), 20 and 8 are number of electron equivalents in a mole of biomass synthesis half reaction (with NH₄⁺ as the N source) and acetate respectively³⁸ and 61 (g/mol) is the molecular weight of acetate.

Scanning Electron Microscopy (SEM). Two intact biofilm-anode samples and naturally detached cells from the outer layers of the biofilm were obtained at the end of one batch MEC experiment (run 2 at 27 days). The two samples were fixed with 4% glutaraldehyde for 12 h at 4 °C and then washed and stored in 10 mM PBS solution. The cell suspension was pasted to a polylysine-coated glass slide for further treatment, whereas the biofilm samples remained intact on the graphite electrode. Both samples were post fixed in 1% osmium tetroxide for 15 min followed by graded-ethanol series dehydration (50%, 70%, 95%, and 100% for 5 min each). This was followed by critical-point drying, after which the samples were mounted on an aluminum stub before being sputter coated with a Au/Pd alloy with a Technics Hummer II sputter coater. We used an FEI XL-30 environmental SEM (Philips) with an accelerating voltage of 5–20 kV and a working distance of 8–10 mm.

RESULTS AND DISCUSSION

Reproducibly High Current Densities in *Thermuncola ferriacetica* Biofilm Anodes. Figure 1 shows that the two batch MECs resulted in exponential current generation within 12–36 h of startup. The maximum current densities (j_{\max}) were 12 and 8.5 A m^{-2} for runs 1 and 2 respectively with sustained current densities of 7.5–8 A m^{-2} for both runs. The high current densities rule out direct contact by a monolayer of cells as the sole EET mechanism for *T. ferriacetica*. Subsequent medium replacements (shown in Figure S1 of the Supporting Information) showed that the current densities quickly rose to the before-replacement values (6–7 A m^{-2}), which supports that *T. ferriacetica* were also not using electron shuttles for EET.

G. sulfurreducens strains genetically modified through directed evolution to produce high current densities, strains KN400 and BEST, produced current densities of ~10 and ~6 A m^{-2} respectively when both strains were grown with 30 mM bicarbonate buffer.^{14,39,40} Maximum and sustained current densities for *T. ferriacetica* that are reported here are the highest reported so far on a planar anode surface for a buffer concentration of 10 mM bicarbonate, and this clearly portrays

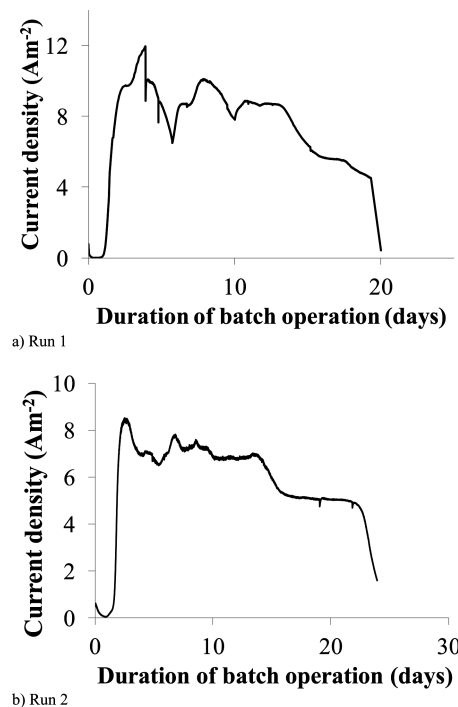


Figure 1. Current density for *T. ferriacetica* as a function of batch MEC operating time for duplicate runs. j_{\max} was $8\text{--}12 \text{ A m}^{-2}$, and a sustained current density around 8 A m^{-2} is evident from both runs.

T. ferriacetica as a model ARB for thermophilic studies. Our previous experiments⁴¹ and modeling through PCBIOFILM^{42,43} show that *G. sulfurreducens* biofilms produce $\sim 3.7 \text{ A m}^{-2}$ with 10 mM HCO_3^- buffer. The diffusion coefficient of HCO_3^- increases by $\sim 87\%$ at the higher temperature (1.53×10^{-5} at 30°C to $2.86 \times 10^{-5} \text{ m}^2/\text{s}$ at 60°C). Thus, the larger diffusion coefficient, coupled with likely faster substrate-utilization kinetics at higher temperature provides a partial explanation for why proton transport was not as important of a limitation within the biofilm anode of *T. ferriacetica*. A high current density with a very low buffer requirement has important implications for applications in organic waste streams with limited buffering capacity. Previous research²¹ with *T. ferriacetica* in an MFC with 10 mM HCO_3^- resulted in j_{\max} and sustained current density of around 0.5 and 0.4 A m^{-2} , respectively; *T. potens* produced around 0.1 A m^{-2} .²³ It is possible that the lack of O_2 in our experiments (MEC operation) helped achieve higher current densities with *T. ferriacetica*. The average CE (and f_c) for the two runs was 93% (91% for run 1 and 95% for run 2); a high CE on acetate is commonly observed with pure-culture ARB, such as *G. sulfurreducens*,^{33,44} and it supports electrons that were not diverted to other sinks such as O_2 .

***T. ferriacetica* Exhibits Fast Growth Rates and Doubling Times.** Growth experiments with a small inoculum size, shown in Figure 2, revealed that exponential growth set in within 12–24 h of MEC startup. The initial exponential phase lasted 36 h, after which the growth entered a linear phase, shown by Figure S2 of the Supporting Information. Assuming that each bacterium generated a similar current at its maximum specific substrate utilization rate (q_{\max}), we can describe the exponential increase in current density by:

$$j = j_0 e^{\mu t} \quad (3)$$

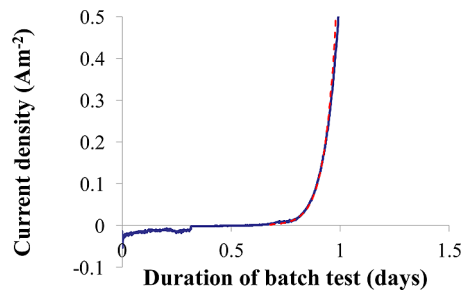


Figure 2. Growth of current density (j) through growth of *T. ferriacetica* on a biofilm anode started with a very small inoculum calculated at the exponential region of the growth curve. The dotted red line corresponds to the model fit according to eq 3.

where j and j_0 represent current densities produced at time t and $t = 0$ respectively and μ is the maximum specific growth rate. A plot of j versus t fits the measured current density well (Figure 2). Previous research has shown that the doubling time for *G. sulfurreducens* was constant during the initial phases of biofilm growth, where current increased exponentially (up to 3 A m^{-2} with a 20% v/v inoculum) as shown in this work.³³ On the basis of the previous ARB growth study, our results with a 1% v/v inoculum resulted in a longer lag time with an exponential increase in current up to 0.3 A m^{-2} , from which we estimated μ for *T. ferriacetica* by taking natural logarithms of eq 3:

$$\ln(j/j_0) = \mu t \quad (4)$$

We plot eq 4 in Figure S3 of the Supporting Information, which gives the slope = μ for the triplicate experiments. The μ value for the *T. ferriacetica* biofilm anode was $17.6 \pm 2.2 \text{ day}^{-1}$, which corresponds to an average doubling time of $1.2 \pm 0.25 \text{ h}$. Thus, *T. ferriacetica* in a biofilm anode grew fast compared to *G. sulfurreducens*, which had an average doubling time of 6 h .³³

Cyclic Voltammetry Reveals a Nernst–Monod Relationship. Figure 3(a) presents the CVs of *T. ferriacetica* under nonlimiting acetate supply. The forward and backward scans have sigmoid shapes that match the Nernst–Monod model with some deviation closer to the maximum current density.^{35,36} The E_{KA} was $-127 \pm 8 \text{ mV}$ (vs SHE), which is $\sim 28 \text{ mV}$ more positive than *G. sulfurreducens* biofilm anodes.^{45–47} The good fitting to the Nernst–Monod model for the *T. ferriacetica* biofilm anodes having high current density is further indication of a solid conductive matrix.⁵ Nernst–Monod behavior has been reported before for *T. ferriacetica*,²¹ but the E_{KA} was -38 mV (vs SHE), a value significantly more positive than reported here. The high E_{KA} value may have been related to interference from O_2 due to MFC operation, the low current density (about 20-fold less than in our study), a large Ohmic loss between the reference electrode and the anode, or a combination.

The baseline-subtracted CV with no acetate, shown in Figure 3(b) for a scan rate of 10 mV s^{-1} (1 mV s^{-1} scan shown in Figure S4 of the Supporting Information), reveals a reversible redox process with a midpoint potential (E_M) of $\sim -0.145 \text{ V}$ (vs SHE). This further confirms that conduction through a solid component of the biofilm is involved in EET for *T. ferriacetica* biofilms. However, it is difficult to determine if this peak corresponds to a single protein or multiple proteins whose responses are inseparable due to relatively close midpoints. We need additional evidence to determine if proteins involved in *T.*

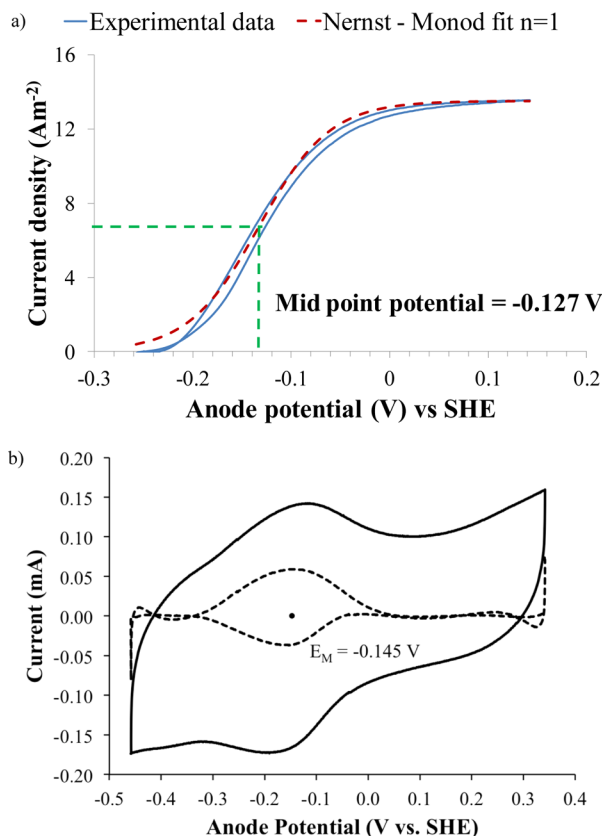


Figure 3. (a) CV scan at 1 mV sec^{-1} on a *T. ferriacetica* biofilm anode performed when it was at its maximum current density (j_{\max}), and the Nernst–Monod model fit for $n = 1$. (b) Raw (black line) and baseline-subtracted (dotted lines) acetate-free CV scan at 10 mV sec^{-1} reveals a midpoint potential of -0.145 V vs SHE of redox proteins possibly involved in EET.

ferriacetica EET are similar to those present in Gram-negative ARB such as *Geobacter* spp. that use a solid conductive matrix for EET. Genome-scale evidence for *T. potens* revealed 32 genes coding for multiheme cytochromes, which are unusual for Gram-positive bacteria.⁴⁸

Kinetic Parameter Estimation for *T. ferriacetica* in a Biofilm Anode. Figure 4(a), which shows CLSM images from a LIVE/DEAD assay on a *T. ferriacetica* biofilm anode, reveals a metabolically active biofilm with an average thickness of $\sim 38 \mu\text{m}$ (100 \times CLSM images shown in Figure S5 of the Supporting Information). Figure 4(b) represents a LIVE/DEAD overlay of $1 \mu\text{m}$ slices (along the Z (depth) axis) from a biofilm section; green (live) cells are present for about $25 \mu\text{m}$, or about 66% of the biofilm thickness. Clearly, multiple layers of cells were active, likely performing EET through a solid conductive matrix. Using the observed biofilm thickness values substituted in eq 1, we calculated a volumetric reaction rate ($q_{\max,\text{app}} X_f$) of $2010 \text{ kg COD m}^{-3} \text{ d}^{-1}$, a value more than two times higher than those calculated for mesophilic ARB such as *G. sulfurreducens*.³⁷

Because $\text{CE} = f_e = 0.93$, the fraction of electrons to biomass synthesis, f_s^o , was 0.07. Y can be calculated from eq 2 giving $0.098 \text{ g vs g COD}^{-1}$ for *T. ferriacetica*, a value lower than that reported for *Geobacter* spp., as shown in Table 1. In summary, we observed a higher $q_{\max,\text{app}} X_f$ and lower Y for *T. ferriacetica* compared to *Geobacter* spp.

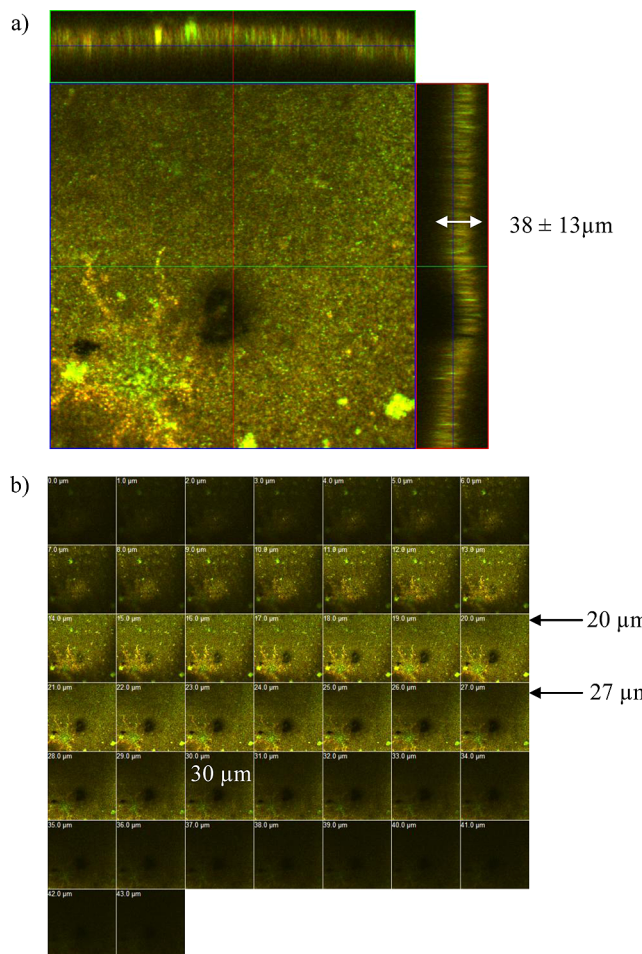


Figure 4. (a) Confocal laser scanning microscope (CLSM) images from a LIVE/DEAD assay of a *T. ferriacetica* biofilm anode showing a section with an average thickness of $38 \pm 13 \mu\text{m}$; (b) $1 \mu\text{m}$ slices of *T. ferriacetica* biofilm section showing the overlaid LIVE/DEAD channels. The presence of green indicates active cells for about $25 \mu\text{m}$ of the whole section, which is evidence indicating multiple active cell layers involved in EET.

Table 1. Summary of Key Kinetic and Electrochemical Parameters for *T. ferriacetica* and *Geobacter* spp

parameter	<i>T. ferriacetica</i>	<i>Geobacter</i> spp.
j_{\max} (A m^{-2})	10 (this study)	8.31^{37}
μ (day^{-1})	0.4^{21}	17.6^{37}
$q_{\max,\text{app}} X_f$ ($\text{kg COD m}^{-3} \text{ d}^{-1}$)	2010 (this study)	1000^{37}
E_{KA} (V vs SHE)	-0.127 (this study)	-0.155^{33}
	-0.038^{21}	-0.150^{13}
		-0.145^{47}
Y (g vs g COD $^{-1}$)	0.098 (this study)	0.14^{37}

Microscopic Structure of *T. ferriacetica* Biofilms Support a Solid Conductive Matrix. SEM micrographs of intact, fixed *T. ferriacetica* in a biofilm anode, shown in Figure 5(a and b), demonstrate a homogeneous stack of straight to slightly curved rods similar to the original isolation study.⁴⁹ These biofilm images contrast with previous studies showing layers of *T. ferriacetica* cells in a densely covered EPS network on an MFC anode²¹ and a single layer of active *T. potens* in a biofilm anode.²³ Naturally detached biofilm cells were fixed on a glass slide, and SEM (part a of Figure S6 of the Supporting

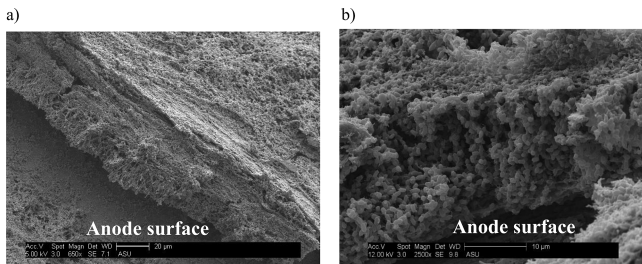


Figure 5. SEM micrographs of *T. ferriacetica* derived from a biofilm anode. The anode surface is clearly labeled in white font to indicate the relative positions. (a) Biofilm fixed on graphite electrode at 650 \times magnification, (b) biofilm fixed on a graphite electrode shows a dense network of cells ($\sim 100 \mu\text{m}$ thick in this section) of homogeneous morphology at 2500 \times magnification. Both images depict multiple layers of stacked cells on the anode surface.

Information) revealed a dense network of extracellular appendages with few cells. Higher magnification (80 000 \times , parts b and c of Figure S6 of the Supporting Information) revealed further structural information on the morphological features of *T. ferriacetica* cells derived from the biofilm anode.

Our study is among the first observations of multiple stacked layers of cells involved in anode respiration for *T. ferriacetica* on a biofilm anode. Additionally, the CLSM images showing an active biofilm of 38 μm thickness, along with the electrochemical Nernst–Monod behavior with high current density, supports that the *T. ferriacetica* biofilms had a solid-conductive matrix to transport electrons to the anode. Thus, the observation of extracellular appendages in *T. ferriacetica* biofilms merits further research regarding their role on anode respiration.

Outlook. Our study is the first documentation that a thermophilic, Gram-positive ARB, *T. ferriacetica*, can produce a high current density, up to 12 A m $^{-2}$ at 60 °C. Multiple lines of evidence point toward EET through a solid conductive matrix by *T. ferriacetica* including: high current density, a thick biofilm ($\sim 38 \mu\text{m}$) with multiple layers of active cells, and Nernst–Monod behavior. Carrying out anode respiration, *T. ferriacetica* has a fast specific growth rate ($\mu = 18 \text{ day}^{-1}$), large volumetric reaction rate ($q_{\max} X_f = 2010 \text{ kg COD m}^{-3} \text{ day}^{-1}$), and low yield ($Y = 0.098 \text{ g VSS g COD}^{-1}$). Furthermore, the high current densities were achieved with a bicarbonate buffer concentration of only 10 mM, which points out the kinetic advantage of thermophilic temperature. Genome sequencing of *T. ferriacetica* currently being carried out as a part of our research efforts in this area should enable the identification of key molecules associated with EET in this microorganism. The identification of efficient thermophilic ARB such as *T. ferriacetica* opens the door for applied research involving biological energy capture from biomass via thermophilic anaerobic food webs.

ASSOCIATED CONTENT

Supporting Information

Figure showing current density response with successive media replacements, figure showing the three phases of the growth experiment along with plot showing the calculation of specific growth rate (μ), nonturnover cyclic voltammogram at 1 mV s $^{-1}$ for *T. ferriacetica* biofilm anode, confocal microscopy images for *T. ferriacetica* biofilm at 100 \times magnification, and scanning electron microscope (SEM) images showing naturally detached cells from the biofilm anode. This material is available free of charge via the Internet at <http://pubs.acs.org>.

AUTHOR INFORMATION

Corresponding Author

*E-mail: prathap@asu.edu; tel: 1-480-727-0849; fax: 1-480-727-0889.

Notes

The authors declare no competing financial interest.

ACKNOWLEDGMENTS

We thank Mr. David Lowry at the Electron microscopy facility at the School of Life Sciences (SoLS) at Arizona State University for his expertise in sample preparation for the SEM. C. I. Torres was supported by the Office of Naval Research Grant No. N000141210344. We thank Mr. Brian Swette for his endowment award to the Swette Center for Environmental Biotechnology, which supported part of the research.

REFERENCES

- (1) Logan, B. E.; Hamelers, B.; Rozendal, R.; Shröder, U.; Keller, J.; Freguia, S.; Aelterman, P.; Verstraete, W.; Rabaey, K. Microbial fuel cells: Methodology and technology. *Environ. Sci. Technol.* **2006**, *40* (17), 5181–5192.
- (2) Call, D.; Logan, B. E. Hydrogen production in a single chamber microbial electrolysis cell lacking a membrane. *Environ. Sci. Technol.* **2008**, *42* (9), 3401–3406.
- (3) Rozendal, R. A.; Leone, E.; Keller, J.; Rabaey, K. Efficient hydrogen peroxide generation from organic matter in a bioelectrical system. *Electrochim. Commun.* **2009**, *11*, 1752–1755.
- (4) Rabaey, K.; Butzer, S.; Brown, S.; Keller, J.; Rozendal, R. A. High current generation coupled to caustic production using a lamellar bioelectrochemical system. *Environ. Sci. Technol.* **2010**, *44*, 4315–4321.
- (5) Torres, C. I.; Marcus, A. K.; Lee, H. S.; Parameswaran, P.; Krajmalnik-Brown, R.; Rittmann, B. E. A kinetic perspective on extracellular electron transfer by anode-respiring bacteria. *FEMS Microbiol. Rev.* **2010**, *34* (1), 3–17.
- (6) Miceli, J. F.; Parameswaran, P.; Kang, D. W.; Krajmalnik-Brown, R.; Torres, C. I. Enrichment and analysis of Anode-Respiring Bacteria from diverse anaerobic inocula. *Environ. Sci. Technol.* **2012**, *46* (18), 10349–10355.
- (7) Parot, S.; Delia, M. L.; Bergel, A. Forming electrochemically active biofilms from garden compost under chronoamperometry. *Bioresour. Technol.* **2008**, *99*, 4809–4816.
- (8) Torres, C. I.; Krajmalnik-Brown, R.; Parameswaran, P.; Marcus, A.; Wanger, G.; Gorby, Y. A.; Rittmann, B. E. Selecting anode respiring bacteria based on anode potential: Phylogenetic, electrochemical, and microscopic characterization. *Environ. Sci. Technol.* **2009**, *43* (24), 9519–9524.
- (9) Nercessian, O.; Parot, S.; Delia, M. L.; Bergel, A.; Achouak, W. Harvesting electricity with *Geobacter bremensis* isolated from compost. *PLoS One* **2012**, *7* (3), e34216.
- (10) Bond, D. R.; Strycharz-Glaven, S. M.; Tender, L. M.; Torres, C. I. On electron transport through *Geobacter* biofilms. *ChemSusChem* **2012**, *5* (6), 1099–1105.
- (11) Marsili, E.; Rollefson, J. B.; Baron, D. B.; Hozalski, R. M.; Bond, D. R. Microbial biofilm voltammetry: Direct electrochemical characterization of catalytic electrode-attached biofilms. *Appl. Environ. Microbiol.* **2008**, *74* (23), 7329–7337.
- (12) Pocaznoi, D.; Erable, B.; Etcheverry, L.; Delia, M. D.; Bergel, A. Towards an engineering-oriented strategy for building microbial anodes for microbial fuel cells. *Phys. Chem. Chem. Phys.* **2012**, *14*, 13332–13343.
- (13) Srikanth, S.; Marsili, E.; Flickinger, M. C.; Bond, D. R. Electrochemical characterization of *Geobacter sulfurreducens* cells immobilized on graphite paper electrodes. *Biotechnol. Bioeng.* **2008**, *99* (5), 1065–1073.
- (14) Nevin, K. P.; Richter, H.; Covalla, S. F.; Johnson, J. P.; Woodard, T. L.; Orloff, A. L.; Jia, H.; Zhang, M.; Lovley, D. R. Power output and columbic efficiencies from biofilms of *Geobacter*

- sulfurreducens comparable to mixed community microbial fuel cells. *Environ. Microbiol.* **2008**, *10* (10), 2505–2514.
- (15) Chen, S.; He, G.; Hu, X.; Xie, M.; Wang, S.; Zeng, D.; Hou, H.; Shröder, U. A three-dimensional ordered macroporous carbon derived from a natural resource as anode for microbial bioelectrochemical systems. *ChemSusChem* **2012**, *5* (6), 1059–1063.
- (16) Carmona-Martinez, A. A.; Harnisch, F.; Kuhlicke, U.; Neu, T. R.; Schröder, U. Electron transfer and biofilm formation of *Shewanella putrefaciens* as function of anode potential. *Bioelectrochemistry* **2012**, DOI: j.bioelechem. 2012.05.002.
- (17) Marsili, E.; Baron, D. B.; Shikhare, I. D.; Coursolle, D.; Gralnick, J. A.; Bond, D. R. *Shewanella* secretes flavins that mediate extracellular electron transfer. *Proc. Natl. Acad. Sci. U.S.A.* **2008**, *105* (10), 3968–3973.
- (18) Lovley, D. R.; Nevin, K. P. A shift in the current: New applications and concepts for microbe-electrode electron exchange. *Curr. Opin. Biotechnol.* **2011**, *22* (3), 441–448.
- (19) Malvankar, N. S.; Lovley, D. R. Microbial nanowires: A new paradigm for biological electron transfer and bioelectronics. *ChemSusChem* **2012**, *5* (6), 1039–1046.
- (20) Mathis, B. J.; Marshall, C. W.; Milliken, C. E.; Makk, R. S.; Creager, S. E.; May, H. D. Electricity generation by thermophilic microorganisms from marine sediment. *Appl. Microbiol. Biotechnol.* **2008**, *78* (1), 147–155.
- (21) Marshall, C. W.; May, H. D. Electrochemical evidence of direct electrode reduction by a thermophilic Gram-positive bacterium, *Thermincola ferriacetica*. *Energy Environ. Sci.* **2009**, *2* (6), 699–705.
- (22) Wrighton, K. C.; Agbo, P.; Warnecke, F.; Weber, K. A.; Brodie, E. L.; DeSantis, T. Z.; Hugenholtz, P.; Andersen, G. L.; Coates, J. D. A novel ecological role of the Firmicutes identified in thermophilic microbial fuel cells. *ISME J.* **2008**, *2* (11), 1146–1156.
- (23) Wrighton, K. C.; Thrash, J. C.; Melnyk, R. A.; Bigi, J. P.; Byrne-Bailey, K. G.; Remis, J. P.; Schichnes, D.; Auer, M.; Chang, C. J.; Coates, J. D. Evidence for direct electron transfer by a gram-positive bacterium isolated from a microbial fuel cell. *Appl. Environ. Microbiol.* **2011**, *77* (21), 7633–7639.
- (24) Ha, P. T.; Lee, T. K.; Rittmann, B. E.; Park, J.; Chang, I. S. Treatment of alcohol distillery wastewater using a Bacteroidetes – dominant thermophilic microbial fuel cell. *Environ. Sci. Technol.* **2012**, *46* (5), 3022–3030.
- (25) Carlson, H. K.; Lavarone, A. T.; Gorur, A.; Yeo, B. S.; Tran, R.; Melnyk, R. A.; Mathies, R. A.; Auer, M.; Coates, J. D. Surface multiheme c-type cytochromes from *Thermincola potens* and implications for respiratory metal reduction by gram-positive bacteria. *Proc. Natl. Acad. Sci. U.S.A.* **2012**, *109* (5), 1702–1707.
- (26) Ren, Z.; Ward, T. E.; Regan, J. M. Electricity production from cellulose in a microbial fuel cell using a well defined binary culture. *Environ. Sci. Technol.* **2007**, *41*, 4781–4786.
- (27) Rezaei, F.; Richard, T. L.; Logan, B. E. Analysis of chitin particle size on maximum power generation, power longevity, and Coulombic efficiency in solid-substrate microbial fuel cells. *J. Power Sources* **2009a**, *192* (2), 304–309.
- (28) Rezaei, F.; Xing, D. F.; Wagner, R.; Regan, J. M.; Richard, T. L.; Logan, B. E. Simultaneous cellulose degradation and electricity production by *Enterobacter cloacae* in a microbial fuel cell. *Appl. Environ. Microbiol.* **2009b**, *75* (11), 3673–3678.
- (29) Aelterman, P.; Freguia, S.; Keller, J.; Verstraete, W.; Rabaey, K. The anode potential regulates bacterial activity in microbial fuel cells. *Appl. Microbiol. Biotechnol.* **2008**, *78* (3), 409–418.
- (30) Parameswaran, P.; Torres, C. I.; Lee, H. S.; Krajmalnik-Brown, R.; Rittmann, B. E. Syntrophic interactions among anode respiring bacteria (ARB) and non-ARB in a biofilm anode: Electron balances. *Biotechnol. Bioeng.* **2009**, *103* (3), 513–523.
- (31) Bird, L. J.; Bonnaffoy, V.; Newmann, D. K. Bioenergetic challenges of microbial iron metabolism. *Trends Microbiol.* **2011**, *19* (7), 330–340.
- (32) Greeley, R. S.; Smith, W. T.; Stoughton, R. W.; Lietzke, M. H. Electromotive force studies in aqueous solutions at elevated temperatures. 1. The standard potential of the silver-silver chloride electrode. *J. Phys. Chem.* **1960**, *64* (5), 652–657.
- (33) Marsili, E.; Sun, J.; Bond, D. R. Voltammetry and growth physiology of *Geobacter sulfurreducens* biofilms as a function of growth stage and imposed electrode potential. *Electroanalysis* **2010**, *22* (7–8), 865–874.
- (34) LaBelle, E.; Bond, D. R. Cyclic voltammetry of electrode-attached bacteria. In *Bio-electrochemical Systems: from Extracellular Electron Transfer to Biotechnological Application*; Integrated Environmental Technology Series; Lens, Ir. Piet, Ed.; Wageningen University: The Netherlands, 2009.
- (35) Marcus, A. K.; Torres, C. I.; Rittmann, B. E. Conduction based modeling of the biofilm anode of a microbial fuel cell. *Biotechnol. Bioeng.* **2007**, *98*, 1171–1182.
- (36) Torres, C. I.; Marcus, A. K.; Parameswaran, P.; Rittmann, B. E. Kinetic experiments for evaluating the Nernst–Monod model for anode-respiring bacteria (ARB) in a biofilm anode. *Environ. Sci. Technol.* **2008**, *42* (17), 6593–6597.
- (37) Lee, H. S.; Torres, C. I.; Rittmann, B. E. Effects of substrate diffusion and anode potential on kinetic parameters for anode respiring bacteria. *Environ. Sci. Technol.* **2009**, *43* (19), 7571–7577.
- (38) Rittmann, B. E., McCarty, P. L. *Environmental Biotechnology: Principles and Applications*; McGraw-Hill: New York, 2001, Chapter 3.
- (39) Yi, H.; Nevin, K. P.; Kim, B. C.; Franks, A. E.; Klimes, A.; Tender, L. M.; Lovley, D. R. Selection of a variant of *Geobacter sulfurreducens* with enhanced capacity for current production in microbial fuel cells. *Biosens. Bioelectron.* **2009**, *24*, 3498–3503.
- (40) Malvankar, N. S.; Tuominen, M. T.; Lovley, D. R. Biofilm conductivity is a decisive variable for high-current-density *Geobacter sulfurreducens* microbial fuel cells. *Energy Environ. Sci.* **2012**, *5*, 5790–5797.
- (41) Torres, C. I.; Marcus, A. K.; Rittmann, B. E. Proton transport inside the biofilm limits electrical current generation by anode-respiring bacteria. *Biotechnol. Bioeng.* **2008**, *100* (5), 872–881.
- (42) Marcus, A. K.; Torres, C. I.; Rittmann, B. E. Evaluating the impacts of migration in the biofilm anode using the PCBIOPFILM. *Electrochim. Acta* **2010**, *55* (23), 6964–6972.
- (43) Marcus, A. K.; Torres, C. I.; Rittmann, B. E. Analysis of a microbial electrochemical cell using the proton condition in biofilm (PCBIOPFILM) model. *Bioresour. Technol.* **2011**, *102* (1), 253–262.
- (44) Bond, D. R.; Lovley, D. R. Electricity production by *Geobacter sulfurreducens* attached to electrodes. *Appl. Environ. Microbiol.* **2003**, *69* (3), 1548–1555.
- (45) Strycharz-Glaven, S. M.; Tender, L. M. Study of the mechanism of catalytic activity of *Geobacter sulfurreducens* biofilm anodes during biofilm growth. *ChemSusChem.* **2012**, *5*, 1106–1118.
- (46) Strycharz, S. M.; Malanoski, A. P.; Snider, R. M.; Yi, H.; Lovley, D. R.; Tender, L. M. Application of cyclic voltammetry to investigate enhanced catalytic current generation by biofilm-modified anodes of *Geobacter sulfurreducens* strain DL1 vs. strain KN400. *Energy Environ. Sci.* **2011**, *4*, 896–913.
- (47) Richter, H.; Nevin, K. P.; Jia, H.; Lowy, D. A.; Lovley, D. R.; Tender, L. M. Cyclic voltammetry of biofilms of wild type and mutant *Geobacter sulfurreducens* on fuel cell anodes indicates possible roles of OmcB, OmcZ, type IV pili and protons in extracellular electron transfer. *Energy Environ. Sci.* **2009**, *2*, 506–516.
- (48) Byrne-Bailey, K. G.; Wrighton, K. C.; Melnyk, R. A.; Agbo, P.; Hazen, T. C.; Coates, J. D. Complete genome sequence of the electricity producing “*Thermincola potens*” strain JR. *J. Bacteriol.* **2010**, *192* (15), 4078–4079.
- (49) Zavarzina, D. G.; Sokolova, T. G.; Tourova, T. P.; Chernyh, N. A.; Kostrikina, N. A.; Bonch-Osmolovskaya, E. A. *Thermincola ferriacetica* sp. nov., a new anaerobic, thermophilic facultatively chemolithoautotrophic bacterium capable of dissimilatory Fe(III) reduction. *Extremophiles* **2007**, *11*, 1–7.